

# PCCP

Accepted Manuscript



This is an *Accepted Manuscript*, which has been through the Royal Society of Chemistry peer review process and has been accepted for publication.

*Accepted Manuscripts* are published online shortly after acceptance, before technical editing, formatting and proof reading. Using this free service, authors can make their results available to the community, in citable form, before we publish the edited article. We will replace this *Accepted Manuscript* with the edited and formatted *Advance Article* as soon as it is available.

You can find more information about *Accepted Manuscripts* in the [Information for Authors](#).

Please note that technical editing may introduce minor changes to the text and/or graphics, which may alter content. The journal's standard [Terms & Conditions](#) and the [Ethical guidelines](#) still apply. In no event shall the Royal Society of Chemistry be held responsible for any errors or omissions in this *Accepted Manuscript* or any consequences arising from the use of any information it contains.

# Revisiting the role of exact exchange for DFT spin-state energetics of transition metal complexes

Mariusz Radoń\*

## Abstract

Effect of the exact exchange on the spin-state energetics of transition metal complexes is revisited with an attempt to clarify its origin and in regard to performance of DFT methods. Typically, by increasing an amount of the exact exchange in an exchange-correlation functional, higher spin states are strongly stabilized with respect to lower spin states. But this is not always the case, as revealed from the presented studies of heme and non-heme complexes, and of metal cations surrounded by point charges. It is argued that the sensitivity of the DFT spin-state energetics to the exact exchange admixture is rooted in the DFT description of the metal–ligand bonding, rather than of the metal-centered exchange interactions. In the typical case, where transition from a lower spin state to a higher spin state involves an electron promotion from a nonbonding to an antibonding orbital, the lower spin state has a more delocalized charge distribution and contains a larger amount of nondynamical correlation energy than the higher spin state. However, DFT methods have problems with describing these two effects accurately. This interpretation allows to explain why the exact exchange admixture has a much smaller effect on the energetics of spin transitions that involve only nonbonding d orbitals.

---

\*Faculty of Chemistry, Jagiellonian University in Kraków, ul. Ingardena 3, 30-060 Kraków, Poland; E-mail: mradon@chemia.uj.edu.pl

# 1 Introduction

Many physical and chemical properties of transition metal complexes dramatically depend on the spin multiplicity of their ground state and possibility of transition to other low-energy spin states<sup>1</sup>. The relative energy of the alternative spin states, so called spin-state energetics, can be obtained from quantum chemical calculations, but to calculate it accurately is still a grand challenge for wave function theory as well as density functional theory (DFT) methods<sup>2</sup>. The DFT spin-state energetics is very sensitive to an approximation used for exchange-correlation functional, and particularly its exchange part (the exchange functional)<sup>3-5</sup>. Due to this effect, the relative energies obtained from different approximate functionals may differ by as much as 10–30 kcal·mol<sup>-1</sup>, often resulting in disagreement of the DFT spin-state energetics with the experimental data<sup>6,7</sup>. Major discrepancies in the DFT spin state energetics are usually found between the results from pure and hybrid functionals<sup>6</sup>. For the latter functionals, the energetics is determined by an amount of the exact exchange included in the functional, as was found in the seminal paper by Reiher *et al.*<sup>8</sup>. A typical behavior<sup>2,6,8,9</sup> is that by increasing the exact exchange admixture a higher spin state (HSS; with a larger number of unpaired electrons) is stabilized with respect to a lower spin state (LSS; with none or a smaller number of unpaired electrons).\*

Although the effect of the exact exchange on the spin-state energetics is rather well established on empirical basis, the author agrees with Harvey that physical effects contributing to this behavior are not completely clear<sup>6</sup>. The usual explanation<sup>6</sup> is by the fact that there are more stabilizing exchange interactions in the HSS than in the LSS, by which the Hartree-Fock method (exact exchange, no correlation)

---

\*The terms: “higher spin state (HSS)” and “lower spin state (LSS)” are preferred in this work over “high-spin state” and “low-spin state,” because some complexes studied here have also an intermediate-spin state. The intermediate-spin state is a LSS when compared with the high-spin state, but a HSS when compared with the low-spin state.

tends to favor the HSS with respect to the LSS<sup>8,10,11</sup>. However, due to the way hybrid functionals are constructed, when adding a given amount of the exact exchange energy, one simultaneously removes the equal amount of an approximate exchange energy. This principle is seen in the construction of the B3LYP-type functional<sup>12</sup>:

$$E_{xc}^{\text{B3LYP}}(x) = xE_x^{\text{exact}} + (1-x)E_x^{\text{Slater}} + 0.72 \cdot \Delta E_x^{\text{B88}} + 0.81 \cdot E_c^{\text{LYP}} + 0.19 \cdot E_c^{\text{VWN}}, \quad (1)$$

where the  $x$  parameter describes mixing between the exact and Slater exchange contributions ( $x = 20\%$  in the original B3LYP<sup>12</sup>,  $x = 15\%$  in the B3LYP\* reparametrization by Reiher *et al.*<sup>8,9</sup>). A similar prescription can also be identified in the construction of other hybrid functionals, such as the half-and-half functional by Becke<sup>7</sup> and the PBE0 functional by Adamo and Barone<sup>7</sup>. As pointed out by Reiher *et al.*<sup>9</sup>, the effect of exact exchange on the spin state energetics is driven by the difference between the exact and approximate exchange energy. Casida *et al.*<sup>13</sup> completed this picture with an observation that increasing the amount of Slater exchange energy in their model functional (containing no exact exchange and no correlation functional) gives rise to stabilization of the LSS with respect to the HSS; this counterintuitive behavior of Slater exchange is also present in gradient-corrected functionals<sup>13</sup>. In view of that, the following question raises naturally: why the local and gradient-corrected exchange functionals, as compared with the exact exchange, tend to stabilize the LSS with respect to the HSS? And: is this just an artifact or maybe there is some physics described by these functionals responsible for such a behavior?

One of these physical effects may be related to competition of exchange stabilization with the metal–ligand bonding interactions in determining the ground spin state, as described by Swart on the example of metallocenes<sup>10</sup>. Moreover, mixing of the exact exchange with an approximate exchange functional is sometimes viewed

as balancing the description of nondynamical correlation<sup>14</sup> and curing the problem with self-interaction error<sup>15,16</sup> (the effects introduced in the approximate exchange functionals, in contrast to the exact exchange<sup>3,6</sup>). While the both effects have a clear connection to bond dissociation energies and description of transitions states, it may be harder to see why they should also affect the spin-state energetics. Nonetheless, having recognized nondynamical correlation errors in the B3LYP calculations, the group of Friesner recently developed localized orbital correction scheme to improve the results for main group<sup>17,18</sup> and transition metal compounds<sup>19,20</sup>, including also the spin-state energetics of octahedral complexes.<sup>20</sup>

The present autor believes that a valuable insight in the above questions can be obtained by understanding exceptional cases for which the typical, large effect of the exact exchange on the DFT spin-state energetics is, surprisingly, not observed. This is usual for main-group compounds<sup>6</sup>, but it also happens (as will be shown) for some transition metal systems. In the previous study of heme complexes, we have identified that relative spin-state energetics are not equally sensitive to the choice of exchange functional, even for closely related systems<sup>21</sup>. More detailed analysis will be presented here for these heme species and other complexes, as well as for simplified models in which the ligands are intentionally omitted and replaced with point charges. Based on these cases studies it will be attempted to understand which physical effects contribute the most to the observed behavior of the DFT spin state energetics. In judging these matters, the DFT results will be supported by insights from multiconfigurational (CASSCF/CASPT2) calculations. Role of metal–ligand bonding will be underlined, as well as DFT problems with description of charge delocalization and nondynamical correlation, whose connection to the spin-state energetics will be elucidated.

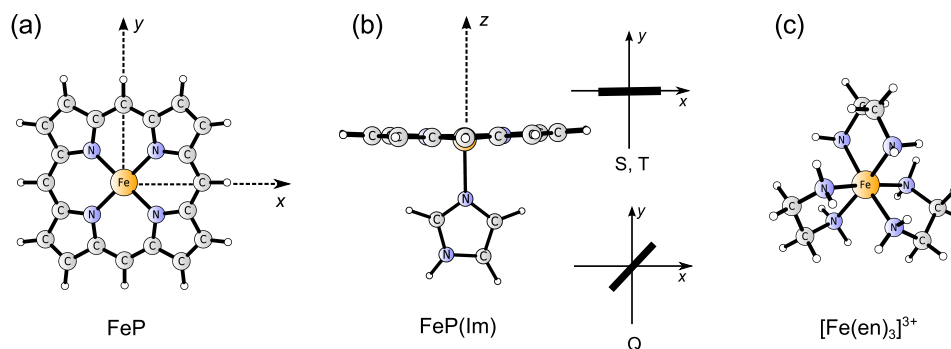


**Figure 1** Structures of heme models FeP (a) and FeP(Im) (b), and complex cation  $[\text{Fe}(\text{en})_3]^{3+}$  (c), where P=porphyrin, Im=imidazole, en=ethylenediamine. Orientation of the imidazole ring for different spin states of FeP(Im) is additionally shown, the porphyrin ring being orientated in the same way as in (a)

## 2 Methodology

Figure 1 gives the structures of models studied in this work:  $\text{Fe}^{\text{II}}\text{P}$  and  $\text{Fe}^{\text{II}}\text{P}(\text{Im})$ , and  $[\text{Fe}^{\text{III}}(\text{en})_3]^{3+}$ , where P=porphyrin, Im=imidazole, en=ethylenediamine; the analogous structure of  $[\text{Cr}^{\text{III}}(\text{en})_3]^{3+}$  is not shown. For the heme models  $[\text{FeP}, \text{FeP}(\text{Im})]$ , the quintet (Q;  $S = 2$ ), triplet (T;  $S = 1$ ) and singlet (S;  $S = 0$ ) spin states are considered. In fact, two close-lying triplets ( $T_1, T_2$ ) as well as an open-shell and closed-shell singlet state ( $S_1, S_2$ ) can be distinguished for FeP. Orbital occupancies of the Fe d orbitals in these spin states are shown in Table 1. For the complexes of Fe(III) and Cr(III), the lowest doublet ( $S = 1/2$ ) and quartet ( $S = 3/2$ ) states are considered. The experimental spin states are: triplet for FeP, quintet for FeP(Im) (see ref. 21 and references therein), doublet for  $[\text{Fe}(\text{en})_3]^{3+}$  and quartet for  $[\text{Cr}(\text{en})_3]^{3+}$  (see ref. 20 and references therein).

For each complex in either spin state the structure has been optimized separately to provide adiabatic relative energies of the spin states. The optimizations were performed at the BP86/def2-TZVP level, with Turbomole<sup>22</sup>. However, for the open-shell singlet ( $S_1$ ) of FeP, the structure of the triplet  $T_1$  state (corresponding to the same electronic configuration) was used. Jahn-Teller distortion for the degenerate

**Table 1** Spin states considered for FeP and FeP(Im)

System	Spin state <sup>a</sup>	Electronic configuration
FeP	Q ( <sup>5</sup> A <sub>1g</sub> )	(d <sub>x<sup>2</sup>-y<sup>2</sup></sub> ) <sup>1</sup> (d <sub>z<sup>2</sup></sub> ) <sup>2</sup> (d <sub>xz</sub> ,d <sub>yz</sub> ) <sup>2</sup> (d <sub>xy</sub> ) <sup>1</sup>
	T <sub>1</sub> ( <sup>3</sup> A <sub>2g</sub> )	(d <sub>x<sup>2</sup>-y<sup>2</sup></sub> ) <sup>2</sup> (d <sub>z<sup>2</sup></sub> ) <sup>2</sup> (d <sub>xz</sub> ,d <sub>yz</sub> ) <sup>2</sup> (d <sub>xy</sub> ) <sup>0</sup>
	T <sub>2</sub> ( <sup>3</sup> E <sub>g</sub> )	(d <sub>x<sup>2</sup>-y<sup>2</sup></sub> ) <sup>2</sup> (d <sub>z<sup>2</sup></sub> ) <sup>1</sup> (d <sub>xz</sub> ,d <sub>yz</sub> ) <sup>3</sup> (d <sub>xy</sub> ) <sup>0</sup>
	S <sub>1</sub> ( <sup>1</sup> B <sub>1g</sub> ) <sup>b</sup>	(d <sub>x<sup>2</sup>-y<sup>2</sup></sub> ) <sup>2</sup> (d <sub>z<sup>2</sup></sub> ) <sup>2</sup> (d <sub>xz</sub> ,d <sub>yz</sub> ) <sup>2</sup> (d <sub>xy</sub> ) <sup>0</sup>
	S <sub>2</sub> ( <sup>1</sup> A <sub>1g</sub> )	(d <sub>x<sup>2</sup>-y<sup>2</sup></sub> ) <sup>2</sup> (d <sub>z<sup>2</sup></sub> ) <sup>0</sup> (d <sub>xz</sub> ,d <sub>yz</sub> ) <sup>4</sup> (d <sub>xy</sub> ) <sup>0</sup>
FeP(Im) <sup>c</sup>	Q ( <sup>5</sup> A')	(d <sub>x<sup>2</sup>-y<sup>2</sup></sub> ) <sup>1</sup> (d <sub>z<sup>2</sup></sub> ) <sup>1</sup> (d <sub>  </sub> ) <sup>2</sup> (d <sub>⊥</sub> ) <sup>1</sup> (d <sub>xy</sub> ) <sup>1</sup>
	T ( <sup>3</sup> A'')	(d <sub>x<sup>2</sup>-y<sup>2</sup></sub> ) <sup>2</sup> (d <sub>z<sup>2</sup></sub> ) <sup>1</sup> (d <sub>  </sub> ) <sup>2</sup> (d <sub>⊥</sub> ) <sup>1</sup> (d <sub>xy</sub> ) <sup>0</sup>
	S ( <sup>1</sup> A')	(d <sub>x<sup>2</sup>-y<sup>2</sup></sub> ) <sup>2</sup> (d <sub>z<sup>2</sup></sub> ) <sup>0</sup> (d <sub>  </sub> ) <sup>2</sup> (d <sub>⊥</sub> ) <sup>2</sup> (d <sub>xy</sub> ) <sup>0</sup>

<sup>a</sup>In parenthesis the term symbol for point group  $D_{4h}$  (FeP) or  $C_s$  (FeP(Im)). <sup>b</sup>The term symbol is given from group-theoretical analysis and comparison with CASSCF calculations. However, once this open-shell singlet state is described by broken-symmetry (BS) formalism, it has undefined symmetry. <sup>c</sup>The d<sub>||</sub> and d<sub>⊥</sub> orbitals are combinations of d<sub>xz</sub> and d<sub>yz</sub> parallel or perpendicular, respectively, to the plane of the Im ring; note that the ring orientation is different for the S,T than for the Q state—thus d<sub>||,⊥</sub> = d<sub>xz,yz</sub> for the S,T states but d<sub>||,⊥</sub> = (d<sub>xz</sub> ± d<sub>yz</sub>)/√2 for the Q state.

triplet state (T<sub>2</sub>) of FeP was taken into account by optimizing its structure under the lower ( $D_{2h}$ ) symmetry.

The optimized structures have been used in subsequent single-point calculations in Gaussian 09<sup>23</sup>, employing the B3LYP-type functional defined by eq. (1) with various values of  $x$  to see how the spin-state energetics depends on it.<sup>†</sup> The basis set for these calculations was composed of cc-pVQZ-DK on the metal and cc-pVTZ-DK on the ligands<sup>25</sup>; the scalar relativistic effects were included up to the second-order Douglas-Kroll-Hess (DKH) level<sup>26</sup>. In addition to standard, self-consistent field (SCF) calculations, the triplet–quintet splitting of FeP was also calculated using the orbitals earlier optimized for a different value of the  $x$  parameter. These non-SCF calculations were carried out by providing the appropriate initial guess and setting to 1 the number of allowed SCF cycles.

<sup>†</sup>Note that using the fixed geometries for B3LYP-type functionals with various  $x$  values is an approximation which is well established in DFT calculations<sup>5,24</sup> and not expected to change the calculated relative energies by more than 0.1–1.0 kcal/mol, thus not affecting the conclusions drawn in this paper. Moreover, by using the same set of structures (here: BP86-optimized) for every  $x$ -value, it is warranted that the effects discussed are purely electronic, i.e., not due to a (small) dependence of the structure on the functional.

In order to highlight the role of metal–ligand bonding, additional calculations were performed for simplistic models in which the central metal ion was surrounded by four or six point charges of  $q = -0.5e$ , intended to mimic either square-planar coordination (in the case of  $\text{Fe}^{2+}$  ion) or octahedral coordination (in the case of  $\text{Fe}^{3+}$ ,  $\text{Cr}^{3+}$  ions). The charges were placed at the distance  $r_0 = 1.131 \text{ \AA}$  from the respective central ion (this particular distance  $r_0$  was taken after the analogous point-charges model developed in ref. 27). For the  $\text{Fe}^{2+}$ -(point charges) model, the analogs of the FeP spin states were identified by occupying the Fe d orbitals accordingly (cf Table 1). Use of symmetry was necessary to distinguish between the two triplet states ( $T_1$ ,  $T_2$ ). Therefore, in order to define a standard orientation of the model, four dummy helium dummy atoms were added at the square corners,  $10 \text{ \AA}$  away from the iron. These atoms were described with a smaller (def2-SVP) basis set. The dummy He atoms were added for purely technical reasons—to make possible the use of symmetry—and obviously play no role for the spin-state energetics.

The DFT calculations for open-shell systems were all spin-unrestricted. This did not lead, however, to a significant spin contamination, except for broken-symmetry solutions that were (intentionally) obtained for the open-shell singlet state of FeP and the open-shell doublet state of  $[\text{Cr}(\text{en})_3]^{3+}$ . The open-shell singlet of FeP was described by broken symmetry (BS) determinant:  $|(d_+)^{\alpha}(d_-)^{\beta}|$ , where  $d_{\pm} = (d_{xz} \pm d_{yz})/\sqrt{2}$ ; this determinant gave a slightly lower energy (by  $\sim 1.5 \text{ kcal}\cdot\text{mol}^{-1}$ ) than the alternative BS determinant:  $|(d_{xz})^{\alpha}(d_{yz})^{\beta}|$ . For a BS state corresponding to a given spin multiplicity  $2S + 1$ , the energy was corrected for spin contamination by applying the approximate projection (AP) scheme<sup>28–30</sup>:

$$E_{2S+1}^{(\text{AP})} = E_{2S+1}^{\text{BS}} - \left( \langle \hat{S}^2 \rangle_{\text{BS}} - S(S+1) \right) \cdot \frac{E_{2S+3} - E_{2S+1}^{\text{BS}}}{\langle \hat{S}^2 \rangle_{2S+3} - \langle \hat{S}^2 \rangle_{\text{BS}}},$$

which removes a spurious contribution to energy from the higher multiplicity state  $2S + 3$ . This formula was applied for  $S = 0$  (open-shell singlet of FeP) and  $S = 1/2$  (open-shell doublet of  $[\text{Cr}(\text{en})_3]^{3+}$ ).

Multiconfigurational CASSCF and CASPT2 calculations for the Q and T<sub>1</sub> spin states of FeP were carried out with Molcas<sup>31</sup>, using the active space of 8 electrons in 11 active orbitals (8in11), described in ref. 21. The calculations employed the ANO-RCC basis set<sup>32</sup>, contracted to: 6s5p3d2f1g for Fe, 4s3p2d1f for N, 3s2p1d for C, and 2s1p for H. Core orbitals below Fe 3s,3p were kept frozen in CASPT2. Scalar relativistic effects were included at the second-order DKH level<sup>26</sup>. The analysis of CASSCF wave function in terms of resonance structures (presented in Table 3) was performed as in ref. 33, after doing a Cholesky localization of the  $\sigma_{xy}, \sigma_{xy}^*$  orbitals (describing the Fe–porphin bond). Contribution of the bond pair  $(\sigma_{xy})^2$  to the correlation energy was estimated by comparing the energies obtained from the (8in11) active space and the (6in10) one in which the  $\sigma_{xy}$  orbital taken from (8in11) calculations was frozen during the CASSCF and CASPT2 calculations, to completely “switch off” the electron correlation for the electron pair occupying  $\sigma_{xy}$ .

### 3 Results and Discussion

Spin-state energetics of heme models, FeP(Im) and FeP, have been studied with a hybrid DFT method defined by eq. (1), where the  $x$  parameter is used to control an amount of the exact exchange included in the functional, ranging from  $x = 0$  (pure gradient-corrected functional) to  $x = 1$  (100%-hybrid functional). Figure 2 shows the resulting energies of selected *spin transitions* (i.e., adiabatic separations between the two involved spin states) as functions of the  $x$  parameter. Two such transitions are distinguished for FeP(Im): the quintet-to-triplet (Q→T) and the triplet-to-singlet (T→S) transition (panel b). For FeP the corresponding transitions

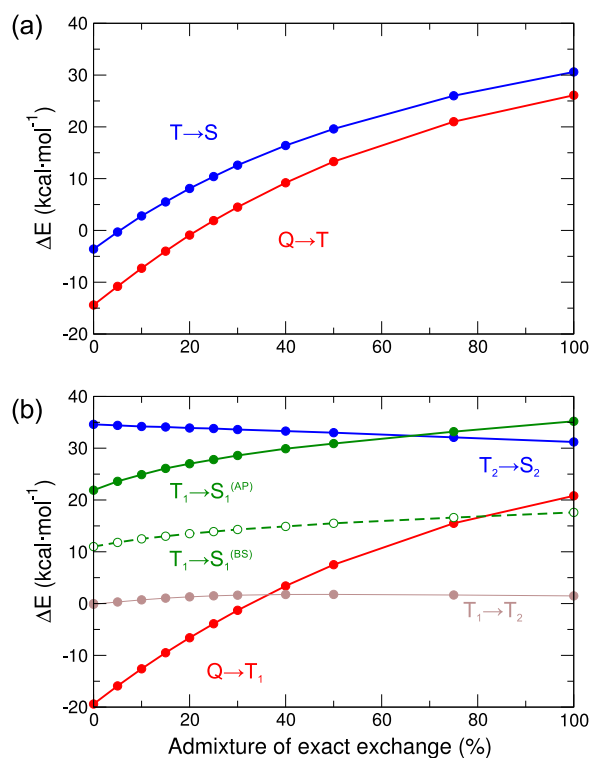


**Figure 2** Energies of selected spin transitions for FeP(Im) (a) and FeP (b) for various admixtures of the exact exchange. The energy of open-shell singlet ( $S_1$ ) for FeP is either from raw broken symmetry (BS) calculations or corrected for spin contamination using the approximate projection (AP) method. *Note that all spin-state energetics are not equally dependent on the admixture of exact exchange*

(analogous in terms of the d orbital occupancies) are:  $Q \rightarrow T_1$  and  $T_2 \rightarrow S_2$  (panel b); their energies are plotted in the same color as for the corresponding spin transitions of FeP(Im). Panel (b) also gives energetics for some other spin transitions in FeP. First, it is shown that separation of the two triplet states ( $T_1$ ,  $T_2$ ) is small and nearly independent on the  $x$  parameter. The energetics of open-shell singlet state ( $S_1$ ) is also given, but will be discussed later on.

Now the main focus is on the  $Q \rightarrow T$  and  $T \rightarrow S$  transitions in FeP(Im) (panel a) and the corresponding transitions  $Q \rightarrow T_1$  and  $T_2 \rightarrow S_2$  in FeP (panel b). The energies of the both spin transitions in FeP(Im) exhibit a strong dependence on the exact exchange admixture ( $x$ ): by increasing the  $x$  parameter: the triplet state is destabilized with respect to the quintet state, and the singlet state is destabilized

with respect to the triplet state. The same behavior is also found for the  $Q \rightarrow T_1$  transition in FeP (panel b, red plot). In fact, the energies for three mentioned transitions are described by very similar functions of  $x$ . In each case, the energy variation is considerable,  $\sim 30\text{--}40 \text{ kcal}\cdot\text{mol}^{-1}$ , of which  $\sim 15 \text{ kcal}\cdot\text{mol}^{-1}$  corresponds to the mostly used range,  $0 \leq x \leq 25\%$ , where the transition energies grow nearly linear with the  $x$  parameter<sup>8,9</sup>. This is consistent with the behavior described in the literature for many transition metal complexes.<sup>3,6,8,10,11</sup> But this is not the case for the  $T_2 \rightarrow S_2$  transition in FeP (panel b, blue plot). This triplet-to-singlet transition really behaves odd, for its energy varies by only  $5 \text{ kcal}\cdot\text{mol}^{-1}$  (as compared with  $30\text{--}40 \text{ kcal}\cdot\text{mol}^{-1}$  discussed above) when the  $x$  parameter grows from 0 to 100%. In fact, the  $T_2 \rightarrow S_2$  energy slightly decreases with growing  $x$ —meaning that in this case the growing admixture of exact exchange gives rise to slight stabilization of the singlet with respect to the triplet state (i.e., opposite to the typical behavior known from the literature).

It is crucial that in terms of the d-orbital occupancies each of the quintet-to-triplet or triplet-to-singlet transitions has the same character for the two systems studied (cf configurations in Table 1). The  $Q \rightarrow T$  transition in FeP(Im) as well as the  $Q \rightarrow T_1$  transition in FeP come down to moving an electron from  $d_{xy}$  into  $d_{x^2-y^2}$ . Likewise, the  $T \rightarrow S$  transition in FeP(Im) as well as the  $T_2 \rightarrow S_2$  transition in FeP come down to moving an electron from  $d_{z^2}$  into one of the two  $d_{xz}, d_{xz}$  orbitals (perpendicular to the P ring and practically nonbonding). In each case the total spin decreases by one unit ( $\Delta S = -1$ ), accordingly with formation of an electron pair in the target orbital. Therefore, the peculiar behaviour of the  $T_2 \rightarrow S_2$  transition in FeP—as compared with the analogous  $T \rightarrow S$  transition in FeP(Im)—must be attributed to different bonding situation in the two complexes, resulting in distinct character of the involved orbitals. Indeed, while the  $d_{xy}$  orbital (i.e., the one depopulated in the  $Q \rightarrow T$ ,  $Q \rightarrow T_1$  transitions) points directly towards the porphyrine nitrogens, hence

it gains an antibonding character for both FeP and FeP(Im), the  $d_{z^2}$  orbital (i.e., the one depopulated in the  $T \rightarrow S$ ,  $T_2 \rightarrow S_2$  transitions) has different character in the two complexes: a  $\sigma^*$  Fe–N<sub>imidazole</sub> antibonding character in the case of FeP(Im), but a nonbonding character in the case of FeP. The other d orbitals involved in the considered spin transitions— $d_{x^2-y^2}$  and  $d_{xz}$ ,  $d_{yz}$  (or they combinations  $d_{\parallel}$ ,  $d_{\perp}$ )—are practically nonbonding for both FeP and FeP(Im).

Therefore, it seems the strong dependence of spin-state energetics on the exact exchange admixture, the effect well known from the literature, is a feature of spin transitions which result in population/depopulation of orbitals with antibonding metal–ligand character. In contrast, it may not be observed for spin transitions involving only nonbonding d orbitals.

Before exploring this observation further, it must be noted that the  $S_2$  state—the closed-shell singlet having the same occupations of the d orbitals as the singlet state of FeP(Im)—is not the lowest singlet state of FeP. The lowest one is open-shell singlet ( $S_1$ ) corresponding to the same electronic configuration as the triplet state  $T_1$  (cf Table 1)<sup>36</sup>. In DFT the  $S_1$  state can be described using the broken-symmetry (BS) formalism, whereas the resulting spin contamination can be corrected by applying the approximate projection (AP) procedure (see Methodology section). The AP-corrected  $T_1 \rightarrow S_1$  transition falls in a good agreement with recent CASPT2 and RASPT2 calculations<sup>35</sup>, which is not the case of the raw BS one. However, either before or after the AP correction, the energetics of the  $T_1 \rightarrow S_1$  transition is not particularly sensitive to the exact exchange admixture; this is consistent with the interpretation above because the  $T_1 \rightarrow S_1$  transition involves only nonbonding orbitals ( $d_{xz}$ ,  $d_{yz}$ ).

Another point is that the  $T_1 \rightarrow S_1$  transition energy is directly related to the effective exchange integral ( $K$ ) between the  $d_{xz}$  and  $d_{yz}$  orbitals. The transition energy equals  $2K$ , when using the AP-corrected energy of the  $S_1$  state, or just (one)

$K$ , when using the raw BS one. From this observation, one can infer that  $K$  is not very sensitive to  $x$ : indeed, it grows by modest  $3 \text{ kcal}\cdot\text{mol}^{-1}$  while changing  $x$  from 0 to 25%, and by further  $3.6 \text{ kcal}\cdot\text{mol}^{-1}$  for  $x$  going up to 100%. While the change of  $K$  is in the expected direction, it is rather too small to explain the effect on the  $Q \rightarrow T_1$  transition energy (even taking into account that the latter transition is accompanied by disappearance of 3 exchange interactions) and definitely too small to explain the great effect observed for the  $T \rightarrow S$  transition in FeP(Im) (likewise, accompanied by disappearance of one exchange interaction).

This slight dependence of the d-d exchange integrals on the admixture of exact exchange can contribute a little to the effects observed in the DFT spin-state energetics, but it does not seem to play a decisive role. Indeed, the  $Q \rightarrow T$  and  $T \rightarrow S$  transition energies for FeP(Im) have nearly the same dependence on  $x$ , despite the different number of exchange interactions destroyed during each transition (i.e., three interactions disappearing during the first transition, only one during the second transition). On the other hand, the closed-shell singlet and the triplet state differ by one exchange interaction both for FeP and FeP(Im); this is not helpful to understand the different behavior of the triplet  $\rightarrow$  singlet transition observed for these two systems.

To better see the role of metal-centered exchange interactions it is also useful to omit the actual ligands completely from the model and thus—in the spirit of crystal field theory—to consider a free  $\text{Fe}^{2+}$  ion surrounded by four negative point charges. The charges are intended to roughly mimic the splitting of the d orbitals due to the square-planar ligand field of the porphyrin (details of the model are described in the Methodology section). For this model one may identify analogues of the FeP electronic states—i.e., having the same occupancies of the 3d orbitals—and to consider the transitions between them (Figure 3). In terms of exchange stabilization, these spin transitions are, in the first approximation, the same as for

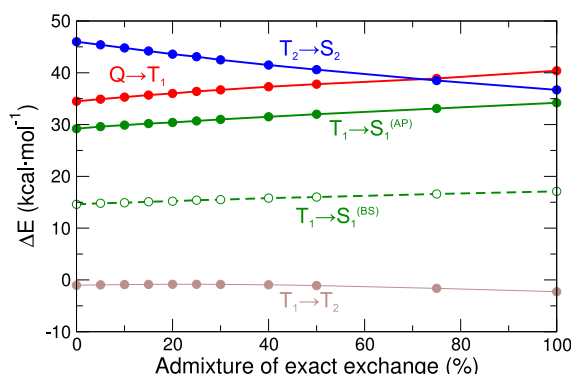


**Figure 3** Energies of selected spin transitions for  $\text{Fe}^{2+}$  ion surrounded by four negative point charges ( $q = -0.5e$  each) for various admixtures of the exact exchange. The energy of open-shell singlet ( $S_1$ ) is either from raw broken symmetry (BS) calculations or corrected for spin contamination using the approximate projection (AP) method

the FeP model; the “only” difference is the absence of metal–ligand bonding. This has, however, profound consequences: for the point charges model the energies of the all spin transitions previously considered ( $Q \rightarrow T_1$ ,  $T_1 \rightarrow S_1$ ,  $T_2 \rightarrow S_2$ ) show only a weak dependence on the  $x$  parameter: either a slight decrease ( $T_2 \rightarrow S_2$ ) or slight increase is observed, but the energy variation with  $x$  is very limited. Thus, the effect of exact exchange on the spin-state energetics in this atomic-like model is clearly different than known for transition metal complexes. Scherlis and Estrin have also found the DFT performance quite different for iron atom and ions than for molecular heme models<sup>37</sup>.

This conclusion—about the crucial role of metal–ligand bonding for the effect of exact exchange on the DFT spin-state energetics—can be supported by further examples from inorganic chemistry. It seems, however, that the most interesting, low-energy spin transitions (e.g., in spin-crossover complexes), necessarily involve population/depopulation of the antibonding orbitals, like the common  $t_{2g} \rightarrow e_g$  transitions in octahedral complexes (where the  $t_{2g}$  orbitals are essentially nonbonding, while the  $e_g$  orbitals have a strong antibonding character). In contrast, spin transitions between the nonbonding  $t_{2g}$  orbitals occur at much higher energy be-

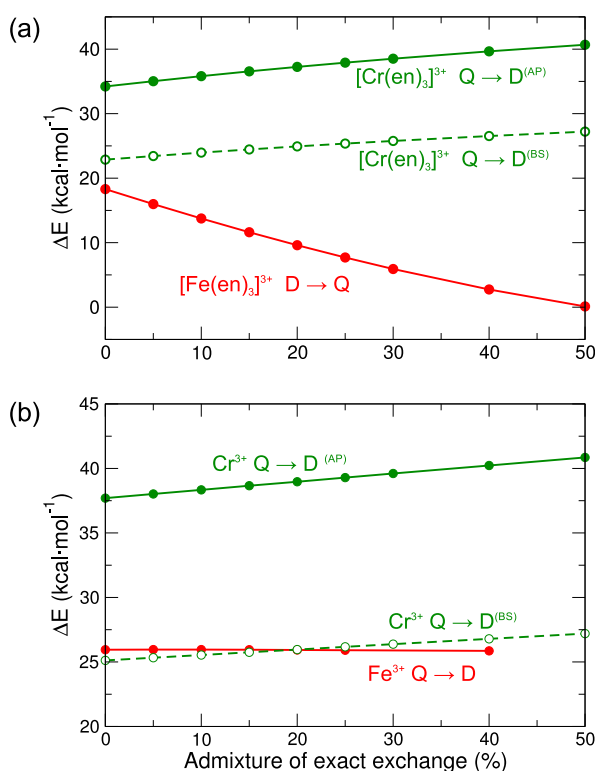


**Figure 4** Spin-state energetics of (a)  $[\text{Fe}(\text{en})_3]^{3+}$  and  $[\text{Cr}(\text{en})_3]^{3+}$  complex cations and (b)  $\text{Fe}^{3+}$  and  $\text{Cr}^{3+}$  ions surrounded by 6 point charges to generate octahedral electrostatic field. Shown are the transition energies between the doublet (D) and quartet (Q) states for various admixtures of the exact exchange. Mind the different energy scale in (a) and (b)

cause the high-spin state is clearly preferred by the exchange interactions in the  $t_{2g}$  manifold<sup>7</sup>. It means that the effects mentioned in this study are easy to overlook.

An example of the  $t_{2g} \rightarrow t_{2g}$  transition is the quartet  $\rightarrow$  doublet one in the  $[\text{Cr}(\text{en})_3]^{3+}$  complex cation. (The doublet state is open-shell, therefore the AP procedure was used to remove the spin contamination.) For comparison, the doublet  $\rightarrow$  quartet transition in  $[\text{Fe}(\text{en})_3]^{3+}$  can be considered; this one involves an electron promotion between the  $t_{2g}$  and  $e_g$  manifolds. As shown in Figure 4(a), the transition energy for the Fe(III) complex is far more (3–4 times) sensitive to the exact exchange admixture than for the Cr(III) complex, although the transitions in the both complexes are between the doublet and quartet state. From a practical point of view, the spin-state energetics in the Cr(III) complex is (within the chemical ac-

curacy) insensitive to the actual value of  $x$ , whereas the one for the Fe(III) complex is very much sensitive—so that its calculation cannot be conclusive without picking a specific value of  $x$ . This was to be expected by comparing the character of orbitals involved in the spin transitions for these two complexes: only nonbonding  $t_{2g}$  orbitals for the Cr(III) complex versus nonbonding  $t_{2g}$  and antibonding  $e_g$  orbitals for the Fe(III) complex. To further support this view, the transitions energies become nearly independent on the  $x$  parameter, once the en ligands are removed and the free ( $\text{Cr}^{3+}$ ,  $\text{Fe}^{3+}$ ) ions embedded in the octahedral electrostatic field—see Figure 4(b).

Another example can be spin-state energetics of metallocenes  $\text{M}(\text{Cp})_2$  (where  $\text{Cp}^-$  is cyclopentadienyl anion, M is divalent first-row transition metal), studied by Reiher *et al.*<sup>9</sup>. In metallocenes the metal d orbitals split into the three levels:  $a'_1(d_{z^2}) < e'_2(d_{xy}, d_{x^2-y^2}) < e''_1(d_{xz}, d_{yz})$  (assuming the  $D_{5h}$  symmetry with the 5-fold axis along the  $z$  direction). The first two levels are nonbonding, while the third level has an antibonding character due to formation of metal–ligand bond with the delocalized  $\pi$  density of the  $\text{Cp}^-$  rings<sup>38</sup>. Accordingly, the spin transitions in early metallocenes (M = Ti, V, Cr) involve only nonbonding orbitals, and the spin-state energetics is much less sensitive to  $x$  than for M = Mn, Fe, in which the spin transitions require an electron promotion between the nonbonding and antibonding d orbitals. In fact, for  $\text{Cr}(\text{Cp})_2$  the increasing admixture of the exact exchange leads to a slight stabilization of the excited singlet state with respect to the triplet ground state<sup>9</sup>—a behavior resembling the  $T_2 \rightarrow S_2$  transition in FeP (see above). In  $\text{V}(\text{Cp})_2$  the relative energy of the doublet and quartet states is nearly  $x$ -independent—in a sharp contrast to a pronounced effect of  $x$  on the energetics of the doublet and quartet states of  $\text{Mn}(\text{Cp})_2$ . It would be very difficult to rationalize these differences only in terms of metal-based exchange interactions: one would have to assume, for instance, that the exchange interactions in V are an order of magnitude less sensitive

**Table 2** Relative energies of the quintet (Q) and triplet ( $T_1$ ) states of FeP<sup>a</sup> obtained using the B3LYP-type functional (1) with  $x = 0\%$  and  $x = 25\%$ , and molecular orbitals self-consistent with either of these two  $x$  values

	orbitals self-consistent with:	
	$x = 0\%$	$x = 25\%$
energetics for:		
$x = 0\%$	19.4	17.2
$x = 25\%$	1.5	3.9

<sup>a</sup>  $E(Q) - E(T_1)$  in kcal·mol<sup>-1</sup>.

to  $x$  than in the case of Mn. On the other hand, the differentiation is very natural based on the bonding situation of the d orbitals in these metallocenes.

At this stage, let us summarize that the large, well-known effect of the exact exchange on spin-state energetics of transition metal complexes must be intimately related to the metal–ligand bonding as it is observed for neither atomic-like models nor spin transitions that involve only nonbonding d orbitals. In accord, the effect does not seem satisfactorily explained in terms of metal-centered exchange interactions.

It is noteworthy that appearance of a metal–ligand bonding induces some delocalization of the d orbitals from the metal toward the ligands, which effectively reduces the exchange interactions in transition metal compounds as compared with free atoms or ions<sup>1</sup>. It is also well known that approximate functionals (LDA, GGA) have a tendency to overestimate electron delocalization; this tendency is partly opposed by introducing exact exchange in hybrid functionals<sup>39,40</sup>. In view of that, it might seem that the effect of exact exchange on the spin state energetics can be simply rationalized by increasing localization of the unpaired electrons on the metal—resulting in greater exchange stabilization of the high-spin state—due to a change of the molecular orbitals with growing the  $x$  parameter. This is, however, not the case as illustrated in Table 2 for the example of the quintet (Q)–triplet ( $T_1$ ) energy difference in FeP. The table compares the relative energies obtained using

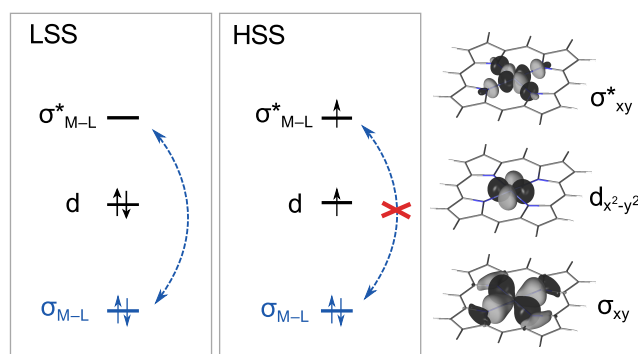


**Figure 5** A scheme of orbital occupancies in the lower spin state (LSS) and the higher spin state (HSS)—for the case of  $\sigma$ -donor ligand and a typical situation when the transition from the LSS to HSS comes down to an electron promotion from the nonbonding d into the antibonding  $\sigma_{M-L}^*$  orbital. Blue dashed arrows show that there is possibility of correlating the electronic pair in  $\sigma_{M-L}$  by means of the  $\sigma_{M-L}^*$  orbital in the LSS, but not in the HSS. The rightmost part shows contour plots of the three considered orbitals in the particular case of FeP, the triplet ( $T_1$ ) being the LSS and the quintet (Q) being the HSS.

the functional given in eq. (1) with  $x = 0$  and  $x = 25\%$ , and molecular orbitals self-consistently optimized for either of these two  $x$  values. As discussed above, inserting the different  $x$  values into the functional point to very different energetics. However, the results are nearly independent on whether the molecular orbitals have been optimized for a given  $x$  value or for the other. Therefore, the effect of the exact exchange on the spin-state energetics is mostly by means of an expression for the exchange-correlation functional, rather than due to varying shape of the molecular orbitals. (This is in agreement with an anecdotal observation in the DFT community that differences between exchange-correlation functionals are usually well reproduced if various approximations to  $E_{xc}[\rho]$  are evaluated for the same electron density; the same was recently pointed out by Cohen *et al.*<sup>40</sup>)

In contrast, all the observations above—concerning the effect of exact exchange admixture on the DFT spin-state energetics—can be more consistently explained if one recalls an impact of the spin state on the metal–ligand bonding. Figure 5 shows schematically occupancies of the key molecular orbitals in a lower spin state (LSS) and a higher spin state (HSS) for a complex with  $\sigma$ -donor ligand(s). This figure refers to the typical case, in which the transition from the LSS to the HSS state involves an

electron promotion from the nonbonding d orbital onto the orbital with an antibonding metal–ligand character, thereby labelled  $\sigma_{M-L}^*$ ; its bonding counterpart is  $\sigma_{M-L}$ . The antibonding  $\sigma_{M-L}^*$  orbital is often, especially in qualitative discussions, called a metal orbital (because it is, indeed, predominantly metal-based) destabilized by interaction with the ligand field. However, the present notation ( $\sigma_{M-L}^*$ ,  $\sigma_{M-L}$ ) emphasizes mixing between the metal and the ligand components, i.e., covalent character of the bond. The rightmost part of Figure 5 depicts the three mentioned orbitals (nonbonding d,  $\sigma_{M-L}$ ,  $\sigma_{M-L}^*$ ) for the example of FeP, where triplet ( $T_1$ ) is the LSS and quintet (Q) is the HSS. Note that the  $\sigma_{xy}^*$  orbital is the orbital that was previously labelled as  $d_{xy}$  (e.g., in Table 1).

The key message is that although no bond is broken during the spin transition, the bond order is lower in the HSS than in the LSS due to an occupation of the antibonding orbital in the HSS. This must, in some sense, weaken the metal–ligand bond in the HSS as compared with the LSS. One effect is that the metal–ligand bond is slightly longer in the HSS in the LSS. However, in the case of macrocycles, such like porphyrin, the metal–ligand distance is largely determined by the structure of the ligand; due to the ligand stiffness it cannot relax very much. Therefore, it is profitable to look also at the electronic aspect of the metal–ligand bond. This can be viewed in two ways.

(1) *An electron donation from the ligand lone pairs to the metal is partly suppressed in the HSS as compared with the LSS.* This is close to the claim of Swart who concluded (based on the energy decomposition analysis) that “metal-ligand bonding is larger for low-spin states than for the higher-spin states due to better suitability of acceptor d-orbitals of the metal in the low spin state”<sup>10</sup>.

A complementary view of this effect can be obtained from the wave function perspective. To this end, it is useful to assess the importance of the ligand-to-metal donation from analysis of a multiconfigurational (CASSCF) wave function in terms

**Table 3** Percentage contributions of resonance structures describing the metal–ligand bonding for the two spin states of FeP estimated from CASSCF calculations with localized active orbitals

Spin state	Weight	Resonance structure
$T_1(^3A_{2g})$	75%	$\text{Fe}^{2+}\text{P}^{2-}$
	19%	$\text{Fe}^{1+}\text{P}^{1-}$
	6%	unidentified <sup>a</sup>
$Q(^5A_{1g})$	92%	$\text{Fe}^{2+}\text{P}^{2-}$
	6%	$\text{Fe}^{1+}\text{P}^{1-}$
	3%	unidentified <sup>a</sup>

<sup>a</sup>Coming from configurations with less than 1% weights, which were not classified in terms of resonance structures.

of localized active orbitals (see Methodology and ref. 33). In this analysis the wave function can be naturally interpreted in terms of resonance structures with well-defined charge distribution on the metal and ligand fragments<sup>33,41,42</sup>. Table 3 gives the weights of the contributing resonance structures for the Q and  $T_1$  spin states of FeP (after localization of the  $\sigma_{xy}$ ,  $\sigma_{xy}^*$  orbitals, yielding a nearly pure  $3d_{xy}$  on Fe and a lone-pair orbital on the porphyrin). As might be expected, two resonance structures dominate. The first one ( $\text{Fe}^{2+}\text{P}^{2-}$ ) agrees with the formal oxidation states assigned to Fe(II) and the porphyrinate anion (2−). On top of this, an admixture of the second resonance structure ( $\text{Fe}^{1+}\text{P}^{1-}$ ) describes the electron donation from the porphyrin to the iron. By inspecting the weights of these two resonance structures one can notice immediately that the electron donation is smaller in the Q than in the  $T_1$  state. In the other words, the Fe–porphyrin bond is more covalent for the LSS ( $T_1$ ) than for the HSS (Q).

The present finding agrees with an earlier observation of de Graaf *et al.*<sup>43</sup>, who also found the ligand-to-metal donation more significant in the LSS than in the HSS for several octahedral complexes of Fe(II). A similar effect can be expected for any transition metal complex with  $\sigma$ -donor ligand(s) if only the spin states (LSS, HSS) differ in an occupation of the nonbonding and the antibonding  $\sigma_{M-L}^*$  orbital, as

depicted in Figure 5. Origin of this effect can be explained as follows. Once the  $\sigma_{M-L}^*$  orbital becomes occupied, the metal contribution in this orbital tends to increase in order to maximize exchange interactions between the spin-like electrons on the metal. Consequently, the ligand contribution must increase in the bonding orbital  $\sigma_{M-L}$ , thus reducing the covalent character of the bond. Therefore, the transition between the spin states cannot be viewed as a mere “spin-flip” on the metal, because it also changes an amount of covalency in the metal–ligand bond. As a result, the LSS is expected to have a more delocalized electron distribution than the HSS. But what does it mean for the effect of exact exchange on the DFT spin-state energetics? Approximate exchange functionals, as opposed to the exact exchange, are known for their charge delocalization error (they overstabilize delocalized charge distributions<sup>40</sup>)—hence their tendency to overstabilize the LSS as compared with the HSS.

(2) *A nondynamical electron correlation connected to the metal–ligand bonding play a greater role for the LSS than for the HSS.* Indeed, as shown in Figure 5, in the LSS the empty  $\sigma_{M-L}^*$  orbital may serve as a correlating orbital for the doubly occupied  $\sigma_{M-L}$ . Admixture of the doubly-excited configuration  $(\sigma_{M-L})^0(\sigma_{M-L}^*)^2$  to the principal one,  $(\sigma_{M-L})^2(\sigma_{M-L}^*)^0$ , correlate the electronic pair in  $\sigma_{M-L}$  very efficiently. This is the same type of correlation as in the stretched  $H_2$  molecule, in analogy of what it can also be called a “left-right” correlation<sup>40,44</sup>. However, in the HSS the  $\sigma_{M-L}^*$  orbital is already singly occupied, thus it can no longer serve as the correlating orbital for the electron pair in  $\sigma_{M-L}$ . Consequently, the nondynamical correlation contributes to stabilization of the LSS with respect to the HSS.

Role of this effect has been described by Pierloot<sup>45</sup> in the context of multiconfigurational complete active space (CASSCF/CASPT2) calculations, where making active the orbital(s) with bonding metal–ligand character is crucial for obtaining the good quality of CASPT2 energetics. In fact, the CASSCF/CASPT2 calculations can

be used here to assess the role of this correlation effect for the relative spin state energetics—on the previously considered example of the spin states of FeP:  $T_1$  (LSS) and Q (HSS). It follows that by freezing the electron pair in  $\sigma_{xy}$ —so that it can be correlated neither in CASSCF nor CASPT2 calculations—the stability of the  $T_1$  state (LSS) with respect to the Q state (HSS) is underestimated by 10 kcal·mol<sup>-1</sup> at the CASSCF level and by 13 kcal·mol<sup>-1</sup> at the CASPT2 level. Therefore, the differential correlation effect is significant.

Approximate functionals are, of course, “not aware” of the multiconfigurational mixing invoked above to rationalize that the LSS gains more from nondynamical correlation than the HSS. Nonetheless, it is known that approximate exchange functionals (the local and gradient-corrected ones) account for nondynamical correlation energy, albeit in a very approximate and imperfect way<sup>3,44,46,47</sup>. The problem is that these functionals effectively overestimate the nondynamical correlation energy near the equilibrium geometry—due to this effect they tend to overbind<sup>48</sup>. On the other hand, it is beneficial that these exchange functionals contain at least some rough treatment of nondynamical correlation, because it is not included in widely used correlation functionals. In this context, mixing the approximate exchange functionals with exact exchange (describing, by definition, no correlation, only pure exchange energy) can be seen as balancing the description of nondynamical correlation<sup>3,14,39</sup>. This interpretation is relevant not only for bond dissociation and transition states (where the role of nondynamical correlation is obvious), but also for description of spin-state energetics. Indeed, by increasing the amount of exact exchange in the exchange-correlation functional, one effectively reduces the amount of nondynamical correlation energy contained in it, which results in destabilization of the LSS with respect to the HSS.

Clearly, the effects (1), (2) operate neither for point-charges models, nor for spin transitions that involve only nonbonding d orbitals. This explains why the

usual, large effect of exact exchange on the spin-state energetics is not observed for these transitions. The both aspects (1) and (2) are also clearly connected to self-interaction error, which is sometimes viewed as a proxy for nondynamical correlation<sup>16,49</sup>. Moreover, the view above also explains why the effect of exact exchange is system specific, i.e., it is rather not possible to find a single value of the  $x$  parameter that works well for complexes with different character of the metal–ligand bond. More covalent bonding requires more nondynamical correlation to be included by taking lower the value of  $x$ . Many DFT benchmarks are based on very covalent systems (e.g., organometallics), for which low values of  $x$  are appropriate, but it seems that the  $x$  values needed to correctly reproduce the correct spin-state energetics of transition metal complexes are highly variable from case to case<sup>?</sup> . ‡

We also recognize that the two aspects (1), (2) are not really independent, as the matter of nondynamical correlation is, in fact, an ability of the method to describe the separation of electrons in the bond pair<sup>39</sup>. However, distinguishing the effects (1), (2) seems to be helpful from a conceptual point of view.

## 4 Conclusions

Case studies of spin-state energetics were presented for selected transition metal systems (heme and nonheme complexes, and metal ions surrounded by point charges instead of ligands). The results were analyzed *vis-à-vis* the key question of the paper: what is the true role of exact exchange in determining the DFT spin-state energetics?

Interestingly, for some of the studied systems the typical effect of the exact exchange admixture on the spin-state energetics (i.e., strong stabilization of the

---

‡ Although thorough comparison with high-level *ab initio* calculations is not the aim of this study, it is valuable to take a look at the recent CASPT2 calculations for FeP(Im) and FeP<sup>34,35</sup>. In order to reproduce the best estimates of the Q→T transition energy in FeP(Im) ( $\approx 4.5$ – $6.5$  kcal/mol)<sup>34</sup> and in the Q→T<sub>1</sub> energy for FeP ( $\approx -1$  kcal/mol)<sup>35</sup>, the  $x$  parameter in eq. (1) should be as large as 30%. However, a much smaller value  $x \approx 10\%$ – $15\%$  is needed to reproduce the estimated T→S transition energy in FeP(Im) ( $\approx 3$ – $4$  kcal/mol)<sup>34</sup>.

high-spin with respect to the low-spin state) was not observed. This behavior can be explained by mostly nonbonding character of the d orbitals involved in these spin transitions, whereas typical spin transitions involve electron promotions between the nonbonding and antibonding orbitals. The importance of various physical effects that may contribute to the observed behavior has been evaluated. It was found that metal-centered exchange interactions (which favor higher-spin states compared with the low-spin state in the spirit of the Hund's rule) are not particularly sensitive to the admixture of exact exchange. Where the sensitivity to exchange functional comes from is the metal–ligand bond. The role of bonding was further highlighted by comparison with simplified models in which the ligands were replaced by point charges.

Trying to better understand the observed phenomena, a connection has been clarified between the DFT spin-state energetics and such important concepts as nondynamical correlation and description of charge delocalization (covalency vs ionicity) in the metal–ligand bond. A typical spin transition (involving an electron promotion from a nonbonding to an antibonding d orbital) cannot be viewed as a mere “spin-flip” on the metal: it was argued that such a transition also modulates the nondynamical correlation energy and the degree of covalency in the metal–ligand bond. As the DFT description of these two effects is critically dependent on the admixture of the exact exchange, the same is also observed for the DFT spin-state energetics. This interpretation explains not only why the DFT spin-state energetics is (typically) so sensitive to the amount of the exact exchange, but also why the optimal amount is system-specific and why the usual sensitivity is not observed for certain spin transitions.

Clearly, many ideas presented here—in particular, those concerning nondynamical correlation energy in DFT<sup>3,44,46,47</sup>—are not new; a major recent contribution comes from the group of Friesner (see Introduction)<sup>17–20</sup>. Nonetheless, it is hoped

that connection of these ideas with the problem of spin states has been clarified by the present work. The discussion above was focused on the most typical case of  $\sigma$ -donor ligands, but we are aware that the situation can be more complicated for ligands with strong  $\pi$ -acceptor properties, and especially for noninnocent ligands, where occurrence of spin contamination can contribute additional difficulties. However, there is recently a tendency to highlighting fundamental issues in DFT by means of simplified models—by which the merit of the problem can be easier pinpointed<sup>40</sup>. All in all, it is nice to see that the DFT limitations in the context of spin-state energetics are basically the same as the general shortcomings of contemporary functionals<sup>40</sup>: problems with description of nondynamical correlation and charge delocalization error. In a sense, there seems to be no additional problem with description of exchange interactions in transition metal complexes.

## Acknowledgments

I am thankful to Prof. J. N. Harvey for the interesting discussion and to Prof. E. Broclawik for valuable comments on the manuscript. This work was partly supported by Ministry of Science and Higher Education, Poland (grant no IP2011 044471) and by Foundation for Polish Science (START program). Supercomputing time from ACK CYFRONET, the PL-GRID infrastructure, and WCSS (grant no. 181) is kindly acknowledged.

## References

- [1] S. Shaik, H. Chen and D. Janardanan, *Nature Chemistry*, 2011, **3**, 19–27.
- [2] M. Swart, *Int. J. Quantum Chem.*, 2013, **113**, 2–7.
- [3] J. N. Harvey, *Annu. Rep. Prog. Chem., Sect. C: Phys. Chem.*, 2006, **102**, 203–226.

- [4] A. Ghosh, *J. Biol. Inorg. Chem.*, 2006, **11**, 712–724.
- [5] J. Conradie and A. Ghosh, *J. Phys. Chem. B*, 2007, **111**, 12621–12624.
- [6] J. N. Harvey, *Struct. Bonding*, 2004, **112**, 151–183.
- [7] T. F. Hughes and R. A. Friesner, *J. Chem. Theory Comput.*, 2011, **7**, 19–32.
- [8] M. Reiher, O. Salomon and B. A. Hess, *Theor. Chem. Acc.*, 2001, **107**, 48–55.
- [9] O. Salomon, M. Reiher and B. A. Hess, *J. Chem. Phys.*, 2002, **117**, 4729–4737.
- [10] M. Swart, *Inorg. Chim. Acta*, 2007, **360**, 179–189.
- [11] M. Swart, *J. Chem. Theory Comput.*, 2008, **4**, 2057–2066.
- [12] P. J. Stephens, F. J. Devlin, C. F. Chabalowski and M. J. Frisch, *J. Phys. Chem.*, 1994, **98**, 11623–11627.
- [13] G. Ganzenmüller, N. Berkaine, A. Fouqueau, M. E. Casida and M. Reiher, *J. Chem. Phys.*, 2005, **122**, 234321.
- [14] J. P. Perdew, M. Ernzerhof and K. Burke, *J. Chem. Phys.*, 1996, **105**, 9982–9985.
- [15] S. Patchkovskii and T. Ziegler, *J. Chem. Phys.*, 2002, **116**, 7806–7813.
- [16] V. Polo, E. Kraka and D. Cremer, *Mol. Phys.*, 2001, **100**, 1771–1790.
- [17] R. A. Friesner, E. H. Knoll and Y. Cao, *J. Chem. Phys.*, 2006, **125**, 124107.
- [18] E. Knoll and R. Friesner, *J. Phys. Chem. B*, 2006, **110**, 18787–18802.
- [19] D. Rinaldo, L. Tian, J. N. Harvey and R. A. Friesner, *J. Chem. Phys.*, 2008, **129**, 164108.
- [20] T. F. Hughes, J. N. Harvey and R. A. Friesner, *Phys. Chem. Chem. Phys.*, 2012, **14**, 7724–7738.

- [21] M. Radoń and K. Pierloot, *J. Phys. Chem. A*, 2008, **112**, 11824–11832.
- [22] TURBOMOLE V6.3 2011, a development of University of Karlsruhe and Forschungszentrum Karlsruhe GmbH, 1989–2007, TURBOMOLE GmbH, since 2007; available from <http://www.turbomole.com>.
- [23] M. J. Frisch, G. W. Trucks, H. B. Schlegel, G. E. Scuseria, M. A. Robb, J. R. Cheeseman, G. Scalmani, V. Barone, B. Mennucci, G. A. Petersson, H. Nakatsuji, M. Caricato, X. Li, H. P. Hratchian, A. F. Izmaylov, J. Bloino, G. Zheng, J. L. Sonnenberg, M. Hada, M. Ehara, K. Toyota, R. Fukuda, J. Hasegawa, M. Ishida, T. Nakajima, Y. Honda, O. Kitao, H. Nakai, T. Vreven, J. A. Montgomery, Jr., J. E. Peralta, F. Ogliaro, M. Bearpark, J. J. Heyd, E. Brothers, K. N. Kudin, V. N. Staroverov, R. Kobayashi, J. Normand, K. Raghavachari, A. Rendell, J. C. Burant, S. S. Iyengar, J. Tomasi, M. Cossi, N. Rega, J. M. Millam, M. Klene, J. E. Knox, J. B. Cross, V. Bakken, C. Adamo, J. Jaramillo, R. Gomperts, R. E. Stratmann, O. Yazyev, A. J. Austin, R. Cammi, C. Pomelli, J. W. Ochterski, R. L. Martin, K. Morokuma, V. G. Zakrzewski, G. A. Voth, P. Salvador, J. J. Dannenberg, S. Dapprich, A. D. Daniels, Å. Farkas, J. B. Foresman, J. V. Ortiz, J. Cioslowski and D. J. Fox, *Gaussian 09, Revision A.1*, Gaussian Inc. Wallingford CT 2009.
- [24] F. Neese, *J. Biol. Inorg. Chem.*, 2006, **11**, 702–711.
- [25] N. B. Balabanov and K. A. Peterson, *J. Chem. Phys.*, 2005, **123**, 064107.
- [26] M. Reiher and A. Wolf, *J. Chem. Phys.*, 2004, **121**, 10945–10956.
- [27] K. Boguslawski, C. R. Jacob and M. Reiher, *J. Chem. Theory Comput.*, 2011, **7**, 2740–2752.
- [28] K. Yamaguchi, F. Jensen, A. Dorigo and K. Houk, *Chem. Phys. Lett.*, 1988, **149**, 537–542.

- [29] K. Yamaguchi, Y. Takahara, T. Fueno and K. Houk, *Theor. Chim. Acta*, 1988, **73**, 337–364.
- [30] H. Isobe, S. Yamanaka, M. Okumura, K. Yamaguchi and J. Shimada, *J. Phys. Chem. B*, 2011, **115**, 10730–10738.
- [31] F. Aquilante, L. De Vico, N. Ferré, G. Ghigo, P.-Å. Malmqvist, P. Neogrády, T. B. Pedersen, M. Pitoňák, M. Reiher, B. O. Roos, L. Serrano-Andrés, M. Urban, V. Veryazov and R. Lindh, *J. Comp. Chem.*, 2010, **31**, 224–247.
- [32] B. O. Roos, R. Lindh, P.-Å. Malmqvist, V. Veryazov and P.-O. Widmark, *J. Phys. Chem. A*, 2005, **109**, 6575–6579.
- [33] M. Radoń, E. Broclawik and K. Pierloot, *J. Phys. Chem. B*, 2010, **114**, 1518–1528.
- [34] S. Vancoillie, H. Zhao, M. Radoń and K. Pierloot, *J. Chem. Theory Comput.*, 2010, **6**, 576–582.
- [35] S. Vancoillie, H. Zhao, V. T. Tran, M. F. A. Hendrickx and K. Pierloot, *J. Chem. Theory Comput.*, 2011, **7**, 3961–3977.
- [36] C. Rovira, K. Kunc, J. Hutter, P. Ballone and M. Parrinello, *J. Phys. Chem. A*, 1997, **101**, 8914–8925.
- [37] D. A. Scherlis and D. A. Estrin, *Int. J. Quantum Chem.*, 2002, **87**, 158–166.
- [38] J. C. Green, *Chem. Soc. Rev.*, 1998, **27**, 263–271.
- [39] J. P. Perdew, A. Ruzsinszky, L. A. Constantin, J. Sun and G. I. Csonka, *J. Chem. Theory Comput.*, 2009, **5**, 902–908.
- [40] A. J. Cohen, P. Mori-Sánchez and W. Yang, *Chem. Rev.*, 2012, **112**, 289–320.
- [41] S. Shaik and H. Chen, *J. Biol. Inorg. Chem.*, 2011, **16**, 841–855.

- [42] N. C. Tomson, M. R. Crimmin, T. Petrenko, L. E. Rosebrugh, S. Sproules, W. C. Boyd, R. G. Bergman, S. DeBeer, F. D. Toste and K. Wieghardt, *J. Am. Chem. Soc.*, 2011, **133**, 18785–18801.
- [43] A. Domingo, M. À. Carvajal and C. de Graaf, *Int. J. Quantum Chem.*, 2010, **110**, 331–337.
- [44] N. C. Handy and A. J. Cohen, *Mol. Phys.*, 2001, **99**, 403–412.
- [45] K. Pierloot, *Mol. Phys.*, 2003, **101**, 2083–2094.
- [46] O. V. Gritsenko, P. R. T. Schipper and E. J. Baerends, *J. Chem. Phys.*, 1997, **107**, 5007.
- [47] Y. He, J. Grafenstein, E. Kraka and D. Cremer, *Mol. Phys.*, 2000, **98**, 1639–1658.
- [48] J. P. Perdew, A. Ruzsinszky, G. I. Csonka, O. A. Vydrov, G. E. Scuseria, V. N. Staroverov and J. Tao, *Phys. Rev. A*, 2007, **76**, 040501.
- [49] J. Olah and J. Harvey, *J. Phys. Chem. A*, 2009, **113**, 7338–7345.